Meteoritics & Planetary Science 40, Nr 11, 1621–1634 (2005)
Abstract available online at http://meteoritics.org

Northwest Africa 1950: Mineralogy and comparison with Antarctic lherzolitic shergottites

Takashi MIKOUCHI

Department of Earth and Planetary Science, Graduate School of Science, University of Tokyo,
7-3-1 Hongo, Bunkyo-ku, Tokyo 113-0033, Japan
*Corresponding author. E-mail: mikouchi@eps.s.u-tokyo.ac.jp

(Received 03 February 2005; revision accepted 22 July 2005)

Abstract–NWA 1950 is a new lherzolitic shergottite recently recovered from Morocco and is the first sample of this group found outside Antarctica. Major constituent phases of NWA 1950 are olivine, pyroxenes, and plagioclase glass ("maskelynite") and the rock shows a two distinct textures: poikilitic and non-poikilitic typical of lherzolitic shergottites. In poikilitic areas, several-millimeter-sized pyroxene oikocrysts enclose cumulus olivine and chromite. In contrast, pyroxenes are much smaller in non-poikilitic areas, and olivine and plagioclase glass are more abundant. Olivine in non-poikilitic areas is more Fe-rich ($Fa_{29–31}$) and shows a narrower distribution than that in poikilitic areas ($Fa_{23–29}$). Pyroxenes in non-poikilitic areas are also more Fe-rich than those in poikilitic areas that show continuous chemical zoning suggesting fractional crystallization under a closed system. These observations indicate that pyroxene in non-poikilitic areas crystallized from evolved interstitial melts and olivine was re-equilibrated with such melts. NWA 1950 shows similar mineralogy and petrology to previously known lherzolitic shergottites (ALH 77005, LEW 88516, Y-793605 and GRV 99027) that are considered to have originated from the same igneous body on Mars. Olivine composition of NWA 1950 is intermediate between those of ALH 77005-GRV 99027 and those of LEW 88516-Y-793605, but is rather similar to ALH 77005 and GRV 99027. The subtle difference of mineral chemistry (especially, olivine composition) can be explained by different degrees of re-equilibration compared to other lherzolitic shergottites, perhaps due to different location in the same igneous body. Thus, NWA 1950 experienced a high degree of re-equilibration, similar to ALH 77005 and GRV 99027.

INTRODUCTION

SNC (shergottites, nakhlites, and chassignite) meteorites are widely believed to have originated from the planet Mars and now commonly referred to as "Martian meteorites." Martian meteorites are important samples that have offered direct clues to understand igneous processes and the mantle composition of the red planet (e.g., McSween 1994, 2002). The total number of Martian meteorites known is constantly increasing with the recent discovery of many Martian meteorite samples from the African and Arabian deserts as well as from Antarctica (Meyer 2003; Russell et al. 2004). Most of these newly discovered specimens are shergottites, which form the largest group of Martian meteorites (Meyer 2003). Shergottites can be further classified into three subgroups: basaltic shergottites, lherzolitic shergottites, and olivine-phyric shergottites (McSween 1994; Goodrich 2002). Olivine-phyric shergottites are the most dominant samples among desert shergottites, although this group is rare among Antarctic Martian meteorites (Goodrich 2002; Meyer 2003). The only Antarctic olivine-phyric shergottite is Elephant Moraine 79001 (EETA79001), which is composed of two distinct lithologies, and one of them (lithology "A") shows an olivine-phyric texture (McSween and Jarosewich 1983). In contrast, lherzolitic shergottites have been recovered only from Antarctica: Allan Hills 77005 (ALH 77005), Lewis Cliff 88516 (LEW 88516), Yamato-793605 (Y-793605), and Grove Mountains 99027 (GRV 99027) (Harvey et al. 1993; Ikeda 1994; Treiman et al. 1994; Mikouchi and Miyamoto 1997; Hsu et al. 2004). Thus, this may be due to sampling heterogeneity between Antarctic and desert Martian meteorites, perhaps because of different fall ages between the samples of two different localities. Although lherzolitic shergottites have not been found outside Antarctica, the

discovery of the first non-Antarctic lherzolitic shergottite from Morocco was recently announced (Russell et al. 2004). It is Northwest Africa 1950 (NWA 1950): two stones weighing 414 g and 383 g. In the Meteoritical Bulletin, brief mineralogy and petrology are given and it is reported that NWA 1950 is similar to ALH 77005, the first known lherzolitic shergottite. Because all the known lherzolitic shergottites show similar petrology and mineralogy (e.g., Ikeda 1994; Harvey et al. 1993; Treiman et al. 1994; Mikouchi and Miyamoto 1997; Hsu et al. 2004), and their crystallization and exposure ages are identical (e.g., Nagao et al. 1997; Morikawa et al. 2001; Borg et al. 2002), they are considered to share the same original source on Mars and arrived on Earth as separate falls (Harvey et al. 1993; Treiman et al. 1994; Wadhwa et al. 1999; Mikouchi and Miyamoto 2000). In spite of these similarities, each sample is slightly different from one another in mineral chemistry and it is believed that this is due to different degrees of re-equilibration (e.g., Harvey et al. 1993; Mikouchi and Miyamoto 2000). Therefore, it is of great interest whether this new meteorite can fit to this story. If this is the case, it is important to know the difference of NWA 1950 from the other lherzolitic shergottites to better understand petrogenesis and formation of this group of Martian meteorites. This will be also helpful to reconstruct the igneous body at which these particular Martian meteorites originated. This paper reports a detailed mineralogical and petrological study of NWA 1950 to understand its crystallization history and to make a comparison with other lherzolitic shergottites.

SAMPLES AND ANALYTICAL TECHNIQUES

I prepared a thin section (~10 × 4 mm) from a small rock chip of NWA 1950 and analyzed it by the following methods. Backscattered electron (BSE) images were taken with a Hitachi S-4500 (field emission gun) scanning electron microscope with energy dispersive spectrometers (EDS) (Department of Earth and Planetary Science, University of Tokyo). Elemental distribution maps were acquired by a JEOL JXA 8900L electron microprobe (University of Tokyo). Accelerating voltage was 15 kV, and the beam current was 60 nA. Quantitative wavelength dispersive analyses were performed on a JEOL JCM 733 mk II (University of Tokyo) microprobe by using natural and synthetic standards. Quantitative microprobe analyses of most phases were obtained at 15 kV accelerating voltage with a beam current of 12 nA. A defocused beam (~10 μm in diameter) and lower probe current (8 nA) were employed for the analysis of plagioclase glass to minimize volatile loss (Mikouchi et al. 1999). For comparison of NWA 1950 with other lherzolitic shergottites, mineral compositional data were derived from Mikouchi and Miyamoto (1997) (Yamato-793605), Mikouchi and Miyamoto (2000) (ALH 77005 and LEW 88516) and Hsu et al. (GRV 99027).

PETROGRAPHY

The thin section studied shows two distinct textures, poikilitic and non-poikilitic (Fig. 1). The non-poikilitic areas look interstitial to pyroxene oikocrysts forming a poikilitic texture. In poikilitic areas, large pyroxene crystals (oikocrysts) enclose rounded olivine grains (~1 mm) and euhedral chromites (approximately a few hundred μm). Both olivine and chromites are usually present as composite grains. The sizes of pyroxene oikocrysts reach up to 5 mm. In poikilitic areas, plagioclase glass (or "maskelynite") is rare and small (up to 100 μm). The pyroxene oikocrysts show broad twinning bands (600 μm wide) probably on (100). It is impossible to locate augite areas in oikocrysts by optical microscope, but the X-ray mapping shows that augite is present as patches within oikocrysts (Fig. 2) or at the edges surrounding oikocrysts. In non-poikilitc areas, olivine, pyroxene, and plagioclase glass are major constituent phases and minor phases include merrillite, ilmenite, Fe sulfide, and rare baddeleyite. The abundance of olivine is larger than those of pyroxenes and plagioclase glass in non-poikilitic areas. The average olivine grain size is 500 μm, while pyroxene and plagioclase glass are usually smaller than 500 μm. Olivines in non-poikilitic areas are angular in shape unlike rounded grains in poikilitic areas, and are slightly larger than those in poikilitic areas. In non-poikilitic areas, pyroxene and plagioclase glass occasionally show intergrown textures. The boundary between the poikilitic and non-poikilitic areas are unclear in many cases (Fig. 2). The overall modal abundances of minerals in the NWA 1950 studied were not measured because the thin section studied is relatively small compared to large grain sizes of constituent phases (e.g., millimeter-sized pyroxene oikocrysts), which may lead to unrepresentative results. There are several pieces of evidence for strong shock metamorphism typical for shergottites (e.g., maskelynitization of plagioclase, mosaic extinction of olivine) (e.g., Bischoff and Stöffler 1992). There is also an area showing a faulted structure, partially melted probably due to friction (Fig. 3), but impact melt pocket was not found in the section studied. All the plagioclase grains are isotropic glass and no birefringent areas were observed. The fractures of the section are often filled with calcite, as in other desert shergottites, due to terrestrial weathering during residence in hot deserts (e.g., Crozaz and Wadhwa 2001). Olivines are brownish green in color and are often altered along their rims and interior fractures. The altered portions are turned into dark brown in color. Magmatic inclusions (~100 μm) are common in olivine grains in both areas and they are often surrounded with radial fractures (Fig. 4). The inclusions typically consist of Al-Ti-rich pyroxene (both low and high-Ca pyroxenes) and Si-rich feldspathic glass. Si-rich feldspathic glass sometimes shows a unique texture that patches of Si-rich glass are present within feldspathic Si-poor glass (Fig. 4).

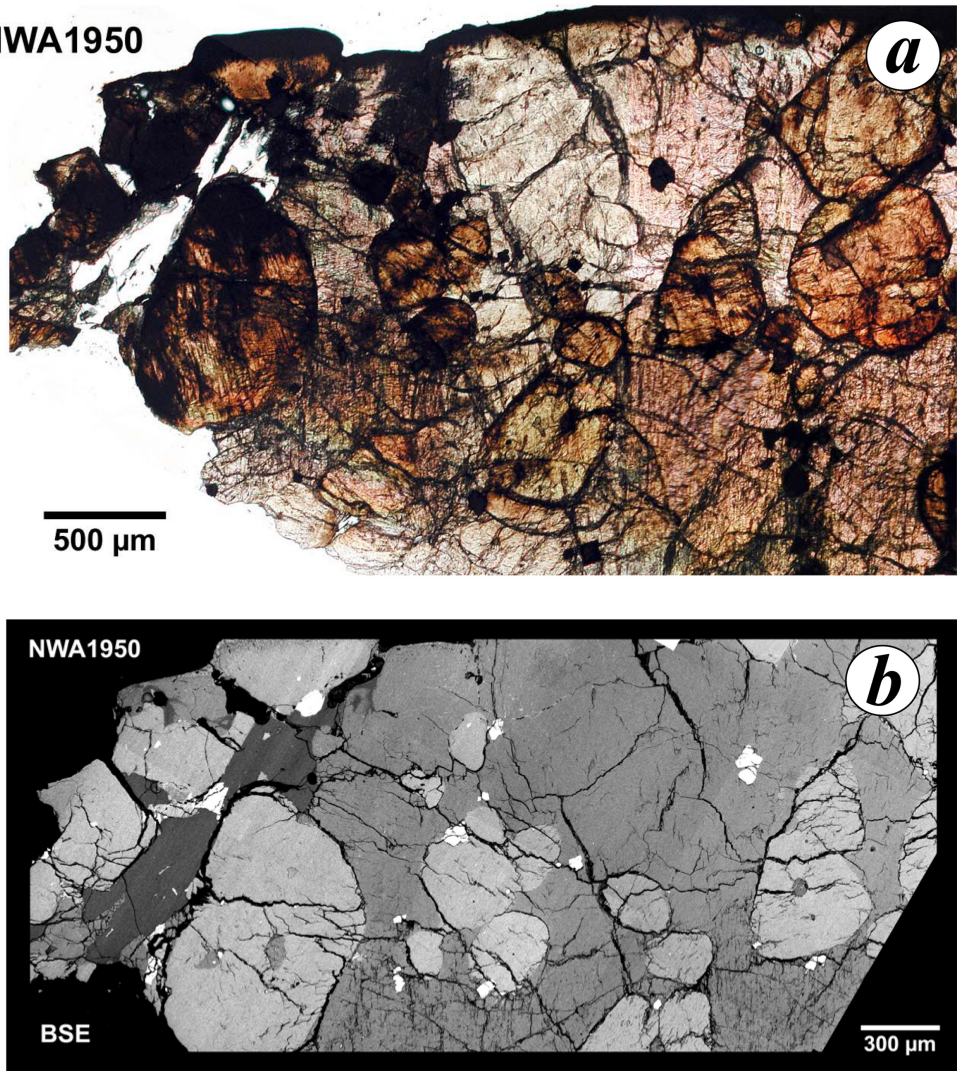

Fig. 1. a) Optical photomicrograph (open nikol) of the NWA 1950 thin section studied. The thin section shows a poikilitic texture mainly composed of a large pyroxene oikocryst enclosing rounded olivine grains and chromite. On the left side of the image, a non-poikilitic area with abundant plagioclase glass (transparent phase) exists. b) A backscattered electron (BSE) image of the NWA 1950 thin section studied (nearly same field of view as Fig. 1a). There are little compositional differences in olivine (~1 mm bright gray phases) and pyroxene (medium gray phases constituting most of the image), respectively, as uniform BSE contrast in each phase shows. Note the presence of magmatic inclusions in olivine grains.

Chromites are usually present as euhedral grains of up to 200 µm in size. The size of chromite in non-poikilitic areas is slightly larger than that in poililitic areas. The abundance of ilmenite is much smaller than that of chromite. The typical size of ilmenite is several tens of µm. Ilmenite is usually associated with chromite. These two opaque minerals are present both in poikilitic and non-poikilitic areas. Merrillite occurs as elongated grains reaching up to 300 µm long. Merrilite is preferentially present in non-poikilitic areas as plagioclase glass.

MINERAL CHEMISTRY

The representative mineral compositions observed in the thin section studied are summarized in Table 1.

Pyroxenes

The pyroxene oikocrysts in poikilitic areas are chemically zoned from Ca-poor cores (near the center of the grain) ($En_{78}Fs_{20}Wo_2$) to a relatively Ca-Fe-rich composition ($En_{66}Fs_{23}Wo_{11}$) at their rims (Fig. 5). The most Ca-poor core is probably orthopyroxene, but electron or X-ray diffraction analysis is required to confirm it. The zoning sequence is continuous and there is little scattering in Fe content compared to Mg and Ca contents. Augite in poikilitic areas are slightly zoned in Ca and Mg contents usually from $En_{54}Fs_{15}Wo_{31}$ to $En_{48}Fs_{14}Wo_{38}$. The pyroxenes in non-poikilitic areas are pigeonite and augite, and no low-Ca pyroxene with $Wo_{<5}$ was found. Pigeonite in non-poikilitic areas is slightly higher in Fe contents than that in poikilitic

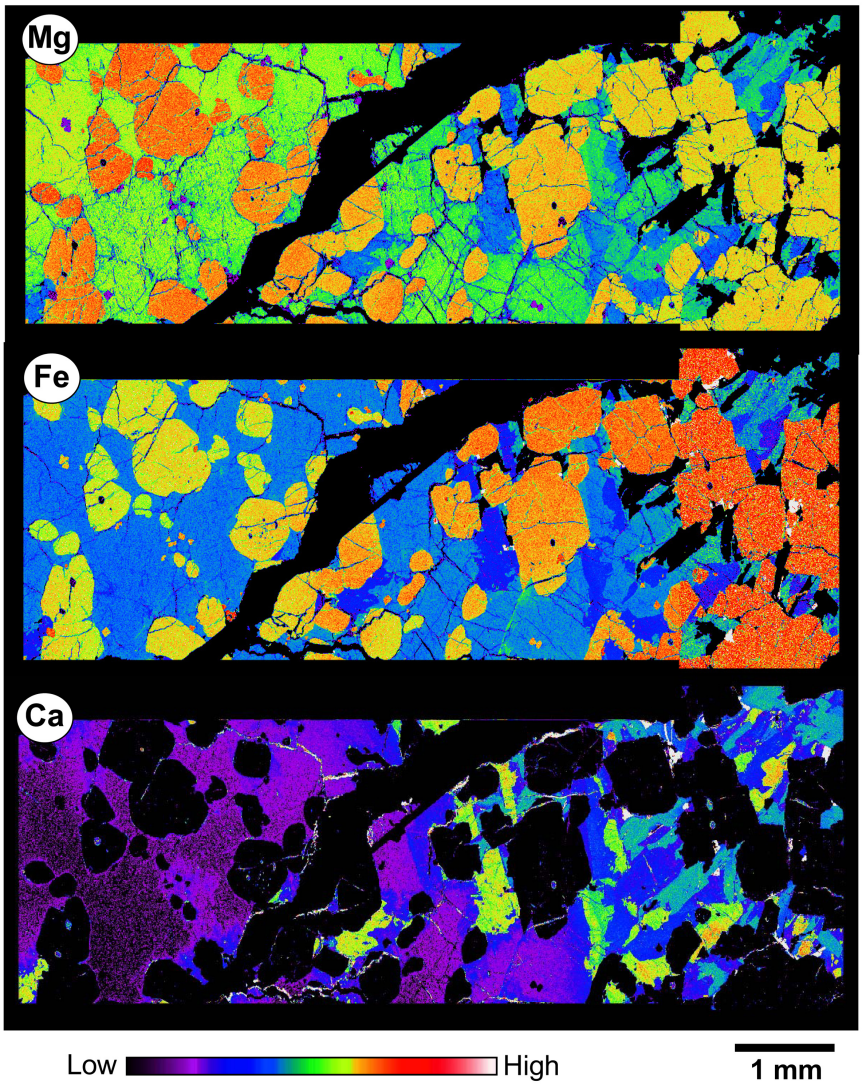

Fig. 2. Mg, Fe, and Ca X-ray compositional maps of NWA 1950. The poikilitic area is present at the left side of the image and the non-poikilitic area is at the right side. The boundary between these two areas is not clear, but located around the center of the image. Mg and Fe maps clearly show that olivine grains in the poikilitic area are more Mg-rich than those in the non-poikilitic area. Augite can be easily identified as yellow to orange grains in the Ca map.

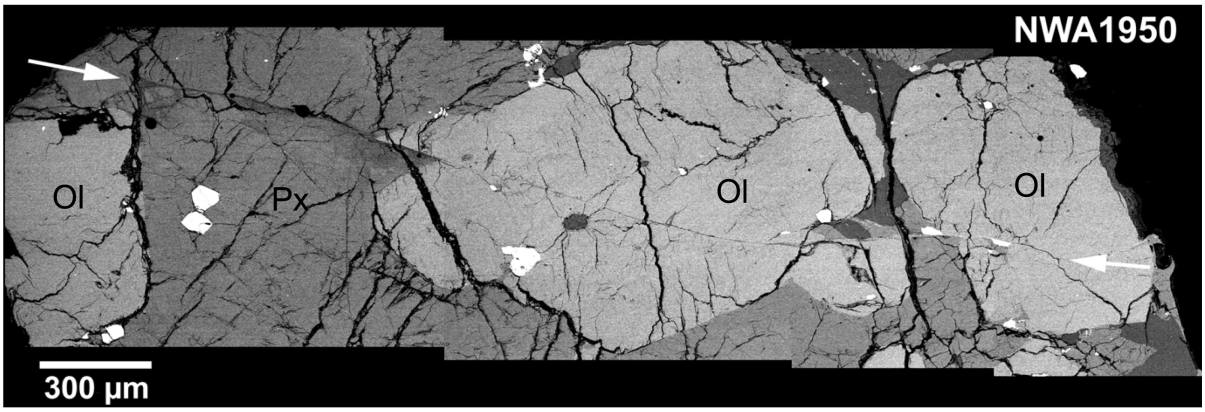

Fig. 3. A BSE image of NWA 1950 showing a thin shock melt vein (indicated by arrows). The olivine grain at the center of the image is clearly faulted along this vein. Ol: olivine. Px: pyroxene.

areas (Fig. 5), although the zoning sequence is not so systematic as that in poikilitic areas. It usually ranges from $En_{67}Fs_{26}Wo_7$ to $En_{63}Fs_{24}Wo_{13}$. Augite in non-poikilitic areas is also slightly more Fe-rich than that in poikilitic areas, ranging from $En_{54}Fs_{15}Wo_{31}$ to $En_{48}Fs_{14}Wo_{38}$. There are clear differences in minor element compositions of pyroxenes between poikilitic and non-poikilitic areas (Fig. 6). TiO_2 of the low-Ca pyroxene in poikilitic areas increases from 0.05 wt% to 0.3 wt%. Al_2O_3 also increases from 0.3 wt% to 0.8 wt%. Both Al and Ti are positively correlated with fe# (atomic Fe/(Fe + Mg)) of pyroxenes. The Ti content of low-Ca pyroxenes in non-poikilitic areas is clearly higher (TiO_2: 0.2~0.7 wt%) than that in poikilitic areas. However, the Al content in non-poikilitic areas shows slightly different behavior. There is a compositional cluster of Al ranging from 1.0–1.4 wt% Al_2O_3 with fe# of 0.25–0.3. There is another cluster of 0.4–0.8 wt% Al_2O_3 and fe# of 0.25–0.3. Cr_2O_3 in the low-Ca pyroxene in poikilitic areas ranges 0.3–0.5 wt% while that in non-poikilitic areas is lower (~0.15 wt%).

Olivine

Olivine in NWA 1950 is fairly uniform in major and minor element composition, but shows a weak compositional variation ranging from Fa_{23} to Fa_{32}. Such a variation is present among different grains, and individual grains are nearly homogeneous (Fig. 2). The olivine grains in poikilitic areas are more magnesian and show wider compositional variation ($Fa_{23–29}$) than those in non-poikilitic areas ($Fa_{29–31}$) (Fig. 7). Especially, in poikilitic areas olivine grains located near the edges of pyroxene oikocrysts generally have more Fe-rich compositions as compared with those near centers of oikocrysts. Minor elements in olivines do not show significant difference between poikilitic and non-poikilitic areas (Fig. 8). CaO contents are 0.1–0.3 wt%. Cr in the NWA 1950 olivine is usually less than 0.05 wt%. Although Ni content in olivine is low, some olivine analysis gave the NiO content of up to 0.1 wt%, suggesting formation under oxidizing condition. Olivine grains attaching to the fusion crust (or shock melt) show reduction of iron producing tiny iron metal (up to a few μm) and Mg-rich olivine (Fig. 9). The chemical composition of such Mg-rich olivine reaches $Fa_{\sim 10}$. A similar texture is observed in pyroxene, but the reduction looks more extensive in olivine.

Plagioclase Glass ("Maskelynite")

Plagioclase glass (maskelynite) in NWA 1950 is weakly zoned in composition. No significant compositional difference can be observed in plagioclase glass between two different areas. The composition typically ranges from $An_{59}Ab_{40}Or_1$ to $An_{47}Ab_{50}Or_3$ (Fig. 10). Minor elements in plagioclase show unique zoning patterns (Fig. 11). FeO decreases from the core to the rim (0.4–0.2 wt%), but then increases (0.2–0.6 wt%). MgO decreases from 0.2 wt% to 0.1 wt% towards the rim.

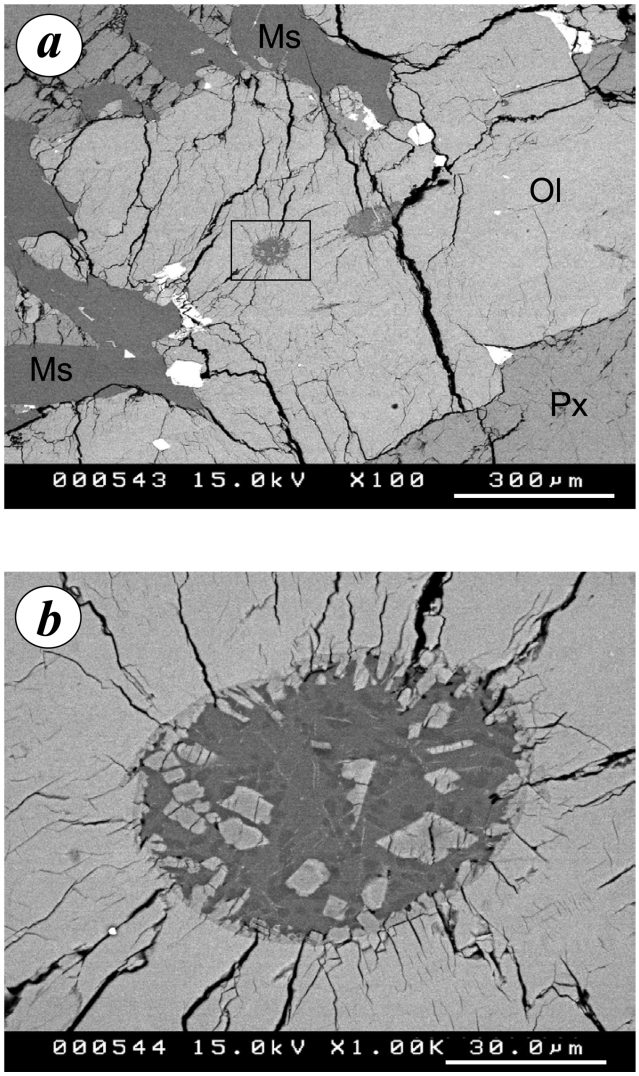

Fig. 4. a) A BSE image of the olivine grain in a non-poikilitic area of NWA 1950. This olivine grain contains two magmatic inclusions. Ol: olivine. Px: pyroxene. Ms: plagioclase glass (maskelynite). b) The enlarged portion shown in (a). This magmatic inclusion is surrounded with radial fractures. Note that several pyroxene grains (Al-Ti-rich) are scattered in two kinds of Si-rich feldspathic glasses. The darker blebs are more Si-rich. The inner wall of the inclusion is rimmed with pyroxene.

Minor Phases

Although chromite in poikilitic areas is rather homogeneous (1 wt% TiO_2, 6 wt% Al_2O_3, 25 wt% FeO, 7 wt% MgO, and 59 wt% Cr_2O_3), that in non-poikilitic areas shows chemical zoning towards the rim of ulvöspinel-rich component (TiO_2 is 1–10 wt% and Cr_2O_3 is 59–38 wt%) (Fig. 12). Ilmenite contains up to 5 wt% MgO. Merrillite contains 3.5 wt% MgO and 1 wt% FeO, respectively. Si-rich

Table 1. Representative mineral compositions of major and minor phases in NWA 1950.

	Poikilitic area						Non-poikilitic area					
	Orthopyroxene	Pigeonite	Augite	Olivine	Maskelynite	Chromite	Pigeonite	Augite	Olivine	Maskelynite	Ti chromite	Merrillite
SiO_2	55.10	53.71	52.66	38.61	57.42	0.08	53.87	52.74	37.19	56.33	0.02	0.09
Al_2O_3	0.32	0.72	1.50	0.01	27.09	5.63	1.38	1.45	0.01	27.50	6.96	0.02
TiO_2	0.08	0.45	0.28	n.d.	0.11	0.85	0.45	0.94	0.03	0.18	9.85	0.00
FeO	13.81	16.29	9.16	20.90	0.59	24.96	15.88	8.87	28.05	0.33	38.01	0.83
MnO	0.48	0.60	0.40	0.42	n.d.	0.43	0.69	0.42	0.50	n.d.	0.70	0.05
MgO	28.01	23.35	17.37	39.20	0.09	6.80	22.15	16.79	34.07	0.10	4.35	3.37
CaO	1.16	4.22	17.03	0.18	9.69	0.02	5.46	17.47	0.25	10.12	0.02	47.06
Na_2O	n.d.	0.09	0.20	0.01	4.49	n.d.	0.10	0.22	0.01	4.98	0.02	1.63
K_2O	n.d.	0.02	0.01	0.01	0.21	n.d.	n.d.	n.d.	0.01	0.24	n.d.	0.05
Cr_2O_3	0.47	0.40	0.69	0.05	n.d.	58.99	0.42	0.92	0.01	n.d.	38.05	0.07
V_2O_3	n.d.	0.12	0.07	0.02	n.d.	0.62	0.08	0.11	0.06	n.d.	0.77	0.02
NiO	0.03	n.d.	n.d.	0.07	0.05	0.02	0.07	0.11	0.02	0.05	0.02	0.11
P_2O_5	0.01	0.05	0.19	0.01	0.14	0.03	0.06	0.15	n.d.	0.13	n.d.	45.58
Total	99.46	100.01	99.55	99.49	99.88	98.43	100.60	100.19	100.21	99.96	98.75	98.85
En	76.6	25.7	14.8				25.5	14.5				
Fs	21.2	65.7	50.0				63.3	48.9				
Wo	2.3	8.5	35.2				11.2	36.6				
Fe#[a]	0.217	0.281	0.228	0.230			0.287	0.229	0.316			
An					53.6					52.1		
Ab					45.0					46.4		
Or					1.4					1.5		

[a]Fe# = atomic Fe/(Fe + Mg). n.d. = not determined.

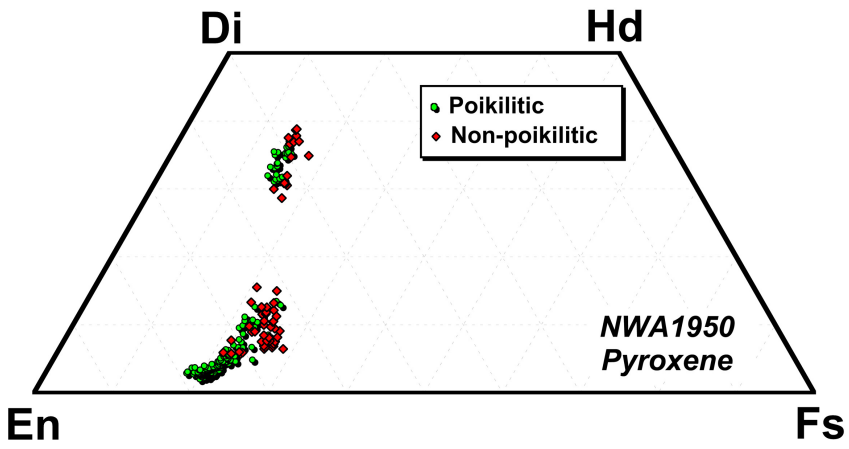

Fig. 5. Pyroxene quadrilateral of NWA 1950 from two different areas. Note that pyroxenes from non-poikilitic areas are slightly more Fe-rich than those from poikilitic areas. Because it is difficult to classify pyroxenes located either in poikilitic or non-poikilitic areas near their boundaries, some analyses are probably overlapped (as there are several pyroxene analyses from non-poikilitic areas that show Mg-rich compositions similar to those in poikilitic areas).

feldspathic glass observed in the magmatic inclusions in olivine can be separated into two groups by silica contents (Fig. 4). One group has about 60 wt% SiO_2 and the other is enriched in SiO_2 (SiO_2: 90 wt%). The presence of two different types of glass with curvilinear boundaries and coalescence textures (Fig. 4b) indicates liquid immiscibility (Harvey et al. 1993). Both low-Ca and high-Ca pyroxenes are observed in magmatic inclusions and they have high Al (Al_2O_3: ~15 wt%) and Ti (TiO_2: ~3.5 wt%) contents.

CRYSTALLIZATION HISTORY OF NWA 1950

NWA 1950 is a rock showing two distinct textures: poikilitic and non-poikilitic, suggesting two different crystallization stages. There is little doubt that olivine and chromite grains in pyroxene oikocrysts are cumulates. Because non-poikilitic areas are interstitial to pyroxene oikocrysts and they are volumetrically minor than poikilitic areas, it is likely that pyroxene oikocrysts themselves are also cumulates. There is no significant compositional and size difference of olivine between poikilitic and non-poikilitic areas (Fig. 2). Olivines in both areas contain similar magmatic inclusions. These observations suggest that olivine in non-poikilitic areas is probably also cumulus. However, olivine in non-poikilitic areas shows a narrower compositional variation and is slightly more Fe-rich than that in poikilitic areas (Fig. 7), implying that olivines in these areas experienced re-equilibration with interstitial melt after accumulation. In contrast, olivine in poikilitic areas was surrounded by a pyroxene oikocryst and had no chance to be highly re-equilibrated. Chromites would have experienced a similar process. Chromites in non-poikilitic areas are zoned towards ulvöspinel-rich compositions at their rims, although their core compositions are similar to those of poikilitic areas (Fig. 12). This is probably due to overgrowth of Ti-rich spinel from evolved interstitial melts in non-poikilitic areas. Pyroxene compositions of non-poikilitic areas are clearly more Ca-, Fe-rich than those of poikilitic areas (Fig. 5). Minor element abundances also show clear differences between pyroxenes in two distinct areas (Fig. 6). It is likely that pyroxenes in non-poikilitic areas crystallized from slightly evolved magma after crystallization of cumulate phases. Continuous chemical zoning of major and minor elements in pyroxene oikocrysts suggests fractional crystallization in a closed system.

Based on the mineralogy of both poikilitic and non-poikilitic areas, the inferred crystallization sequence of minerals observed in NWA 1950 was as follows: First, initial crystallization of olivine and chromite occurred from the parent magma. After crystallization of these phases, low-Ca pyroxenes crystallized in a closed system as products of progressive fractional crystallization and grew into large oikocrysts, poikilitically enclosing olivine and chromite. The crystallizing pyroxene was replaced by augite at some point during growth as oikocrysts. Eventually, small interstitial melts were left between large pyroxene oikocrysts, olivine and chromite. Pigeonite and plagioclase began to co-crystallize from these evolved interstitial melts at first as suggested from an intergrowth texture of pigeonite and plagioclase glass in non-poikilitic areas and formed non-poikilitic textures along with cumulus olivine and chromite. Small amounts of augite then formed and Ti-rich spinel overgrew on cumulus chromite. Because of residence in interstitial melts, cumulus olivine in non-poikiliitc areas experienced re-equilibration, becoming more Fe-rich, and showed a narrower compositional distribution than those of poikilitic areas. Because olivine in pyroxene oikocrysts preserves chemical zoning, it is believed that the effect of re-equilibration was minor after solidification of the NWA 1950 whole rock.

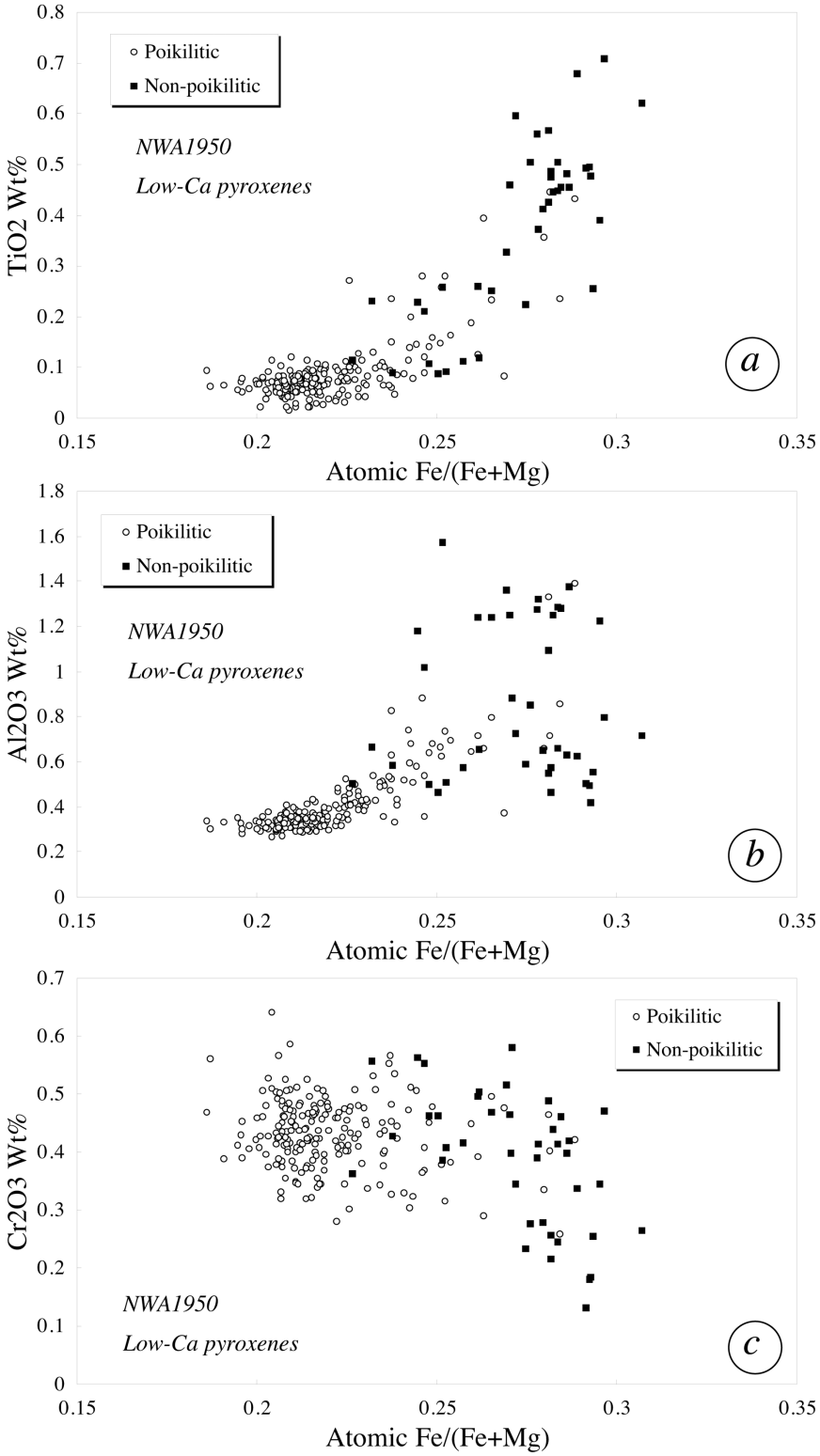

Fig. 6. Variations of (a) Ti, (b) Al, and (c) Cr versus fe# of low-Ca pyroxenes in NWA 1950. Ti and Al abundances in non-poikilitic pyroxenes are higher than those in poikilitic pyroxenes, but Cr abundance shows different behavior. Because it is difficult to distinguish between poikilitic and non-poikilitic areas at their boundaries, some analyses would be overlapped. Probably, some “poikilitic” pyroxenes plotted in the “non-poikilitic” pyroxenes areas are from non-poikilitic areas.

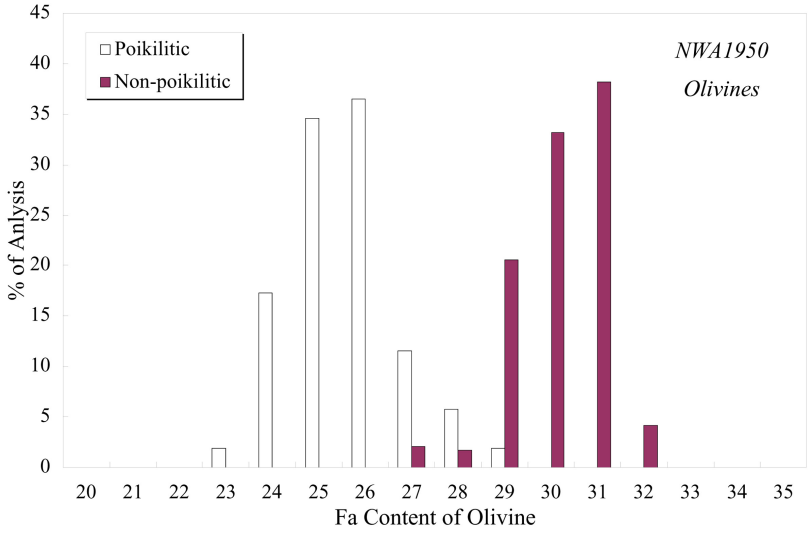

Fig. 7. Fayalite compositional distribution of olivine in NWA 1950. Olivines from non-poikilitic areas show a wider compositional distribution (and more Fe-rich) than those from poikilitic areas.

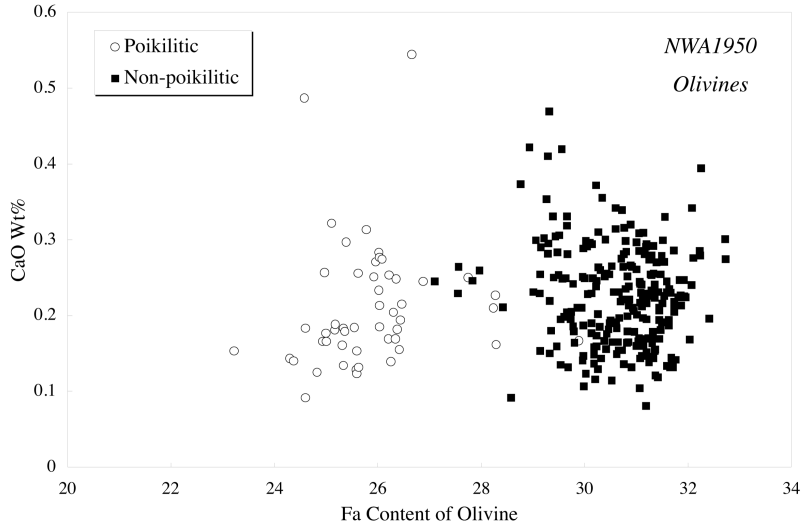

Fig. 8. Ca and fayalite content variations in olivine from NWA 1950. It is obvious that olivines in non-poikilitic areas are more Fe-rich, but Ca content is not so different between two areas.

COMPARISON WITH ANTARCTIC LHERZOLITIC SHERGOTTITES

NWA 1950 is the fifth member of lherzolitic shergottites and is the first sample of this group found outside Antarctica. The recovery of NWA 1950 from northern Africa rules out the possibility that it is paired with any of other lherzolitic shergottites, all of which were discovered in Antarctica. The mineralogy and inferred crystallization history of NWA 1950 that were demonstrated in the previous chapters are generally similar to those of other lherzolitic shergottites (e.g., Harvey et al. 1993; Mikouchi and Miyamoto 2000). However, a detailed comparison of NWA 1950 mineral compositions with other samples provides a clearer position of this sample among lherzolitic shergottites that possibly originated from the same igneous body on Mars. The obtained cosmic-ray exposure ages of Antarctic lhrzolitic shergottites indicate that they were ejected from Mars by the same impact event (Eugster and Polnau 1997; Nagao et al. 1997) and reached different places in Antarctica as different falls (Nishiizumi and Caffee 1997). Such a relationship of lherzolitic shergottites is similar to that observed in nakhlites (e.g., Wadhwa et al. 1999). As previous petrological and mineralogical studies of lherzolitic shergottites suggest that all the samples of this group show similar mineralogy and petrology, but each sample is slightly different from one

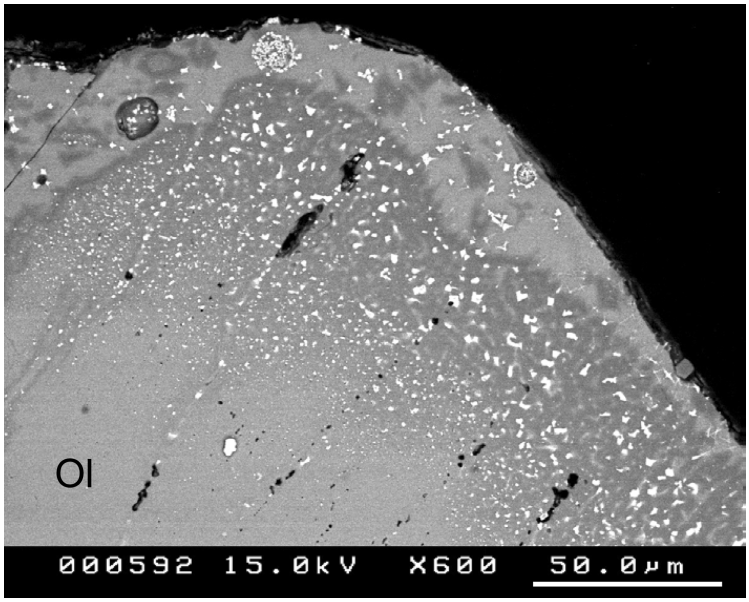

Fig. 9. A BSE image of the olivine grain adjacent to the fusion crust (or impact melt). Note the presence of tiny Fe-metal grains scattered near the rims. In these areas, olivine is more Mg-rich as the BSE image shows darker olivine brightness. Ol: olivine.

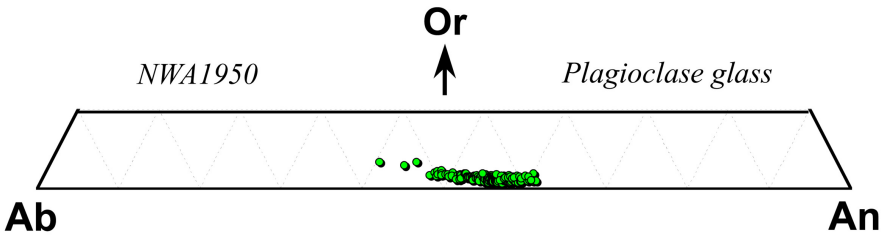

Fig. 10. Plagioclase (glass) compositions of NWA 1950. The compositions of plagioclase glass in other lherzolitic shergottites overlap that of NWA 1950.

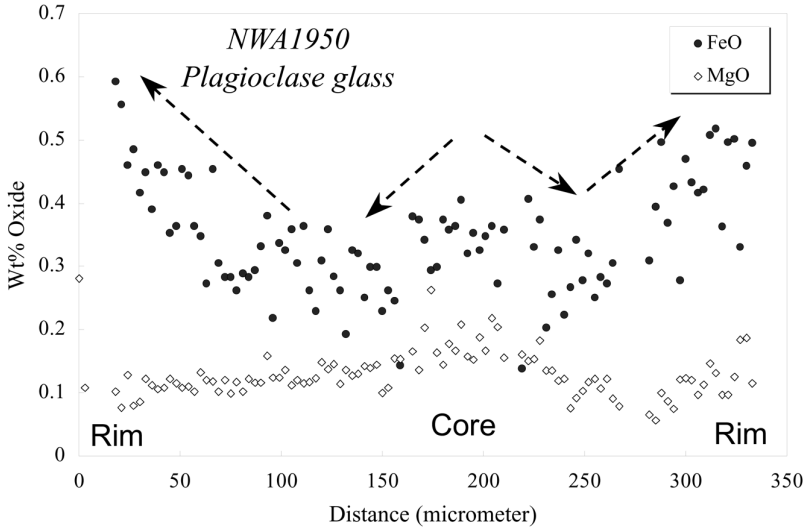

Fig. 11. Fe and Mg zoning patterns in plagioclase glass from NWA 1950. Note that both Fe and Mg show decrease first and then increase from the core to the rim.

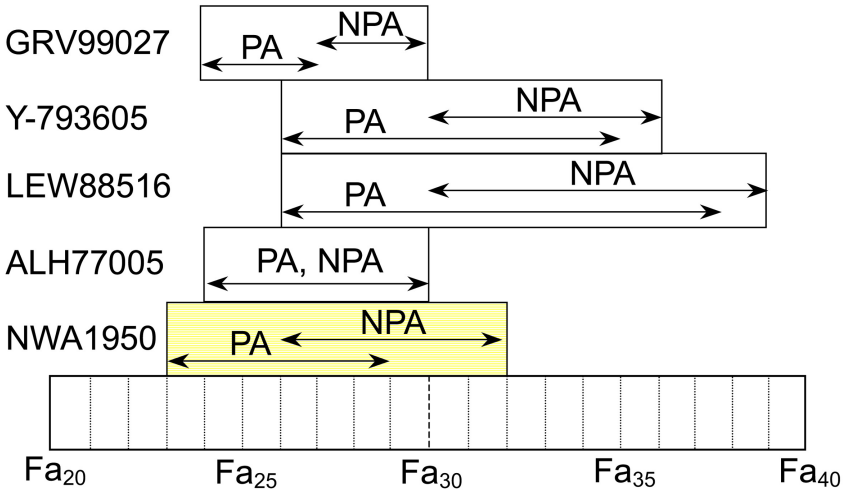

Fig. 13. Olivine compositional variations of lherzolitic shergottites. PA: poikilitic area. NPA: non-poikilitic area.

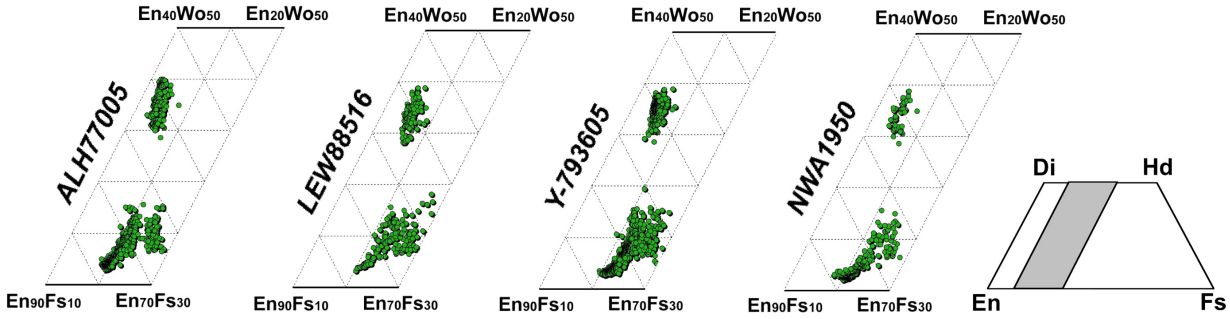

Fig. 14. Pyroxene compositional variations of lherzolitic shergottites.

another in mineral compositions, that are interpreted as different degrees of re-equilibration (e.g., Harvey et al. 1993; Mikouchi and Miyamoto 2000). It is proposed that ALH 77005 and GRV 99027 experienced higher degrees of re-equilibration than LEW 88516 and Y-793605 (e.g., Harvey et al. 1993; Mikouchi and Miyamoto 2000; Hsu et al. 2004). Olivine is a good marker to estimate degrees of re-equilibration because cation diffusion rates (e.g., Fe-Mg) in olivine are faster than those in other major minerals (e.g., Misener 1974; Fujino 1990) (Fig. 13). Olivines in ALH 77005 show a tight compositional distribution around $Fa_{24–30}$ and no compositional difference is observed between poikilitic and non-poikilitic areas. Hsu et al. (2004) reported that GRV 99027 olivine has a similar compositional range of $Fa_{24–30}$ although olivines in poikilitic areas ($Fa_{24–27}$) are slightly more Mg-rich than those in non-poikilitic areas ($Fa_{27–30}$). They suggested that uniform mineral compositions (major and REE elements) of GRV 99027 indicate that it is the most re-equilibrated sample among the previously known lherzolitic shergottites (Hsu et al. 2004). In contrast, olivines in poikilitic areas of LEW 88516 and Y-793605 show clear chemical zoning in individual grains, suggesting lower degrees of re-equilibration. Also, olivines in non-poikilitic areas of these two samples have wider compositional distributions and are more Fe-rich than those in poikilitic areas. Thus, the olivine compositional variation of NWA 1950 ($Fa_{23–32}$) is intermediate between the more homogeneous samples (ALH 77005 and GRV 99027) and the more heterogeneous samples (LEW 88516 and Y-793605). However, the most magnesian olivine composition (Fa_{23}) of NWA 1950 is the most magnesian among the lherzolitic shergottite olivines. Although there is little difference in pyroxene compositions (both in major and minor elements) between NWA 1950 and other lherzolitic shergottites, the most magnesian pyroxene of NWA 1950 ($En_{78}Fs_{20}Wo_2$) is also the most magnesian among lherzolitic shergottites (Fig. 14). This is probably because slower Fe and Mg diffusion rates in pyroxene compared to olivine did not affect their original pyroxene compositions even though each sample experienced different degree of re-equilibration. However, difference in degrees of re-equilibration was significant enough to produce differences in olivine compositions. Similar to pyroxenes, there is no clear difference in plagioclase and spinel compositions between NWA 1950 and other lherzolitic shergottites. Especially, it is noted that minor elements in plagioclase glass from these lherzolitic shergottites show very similar zoning patterns to

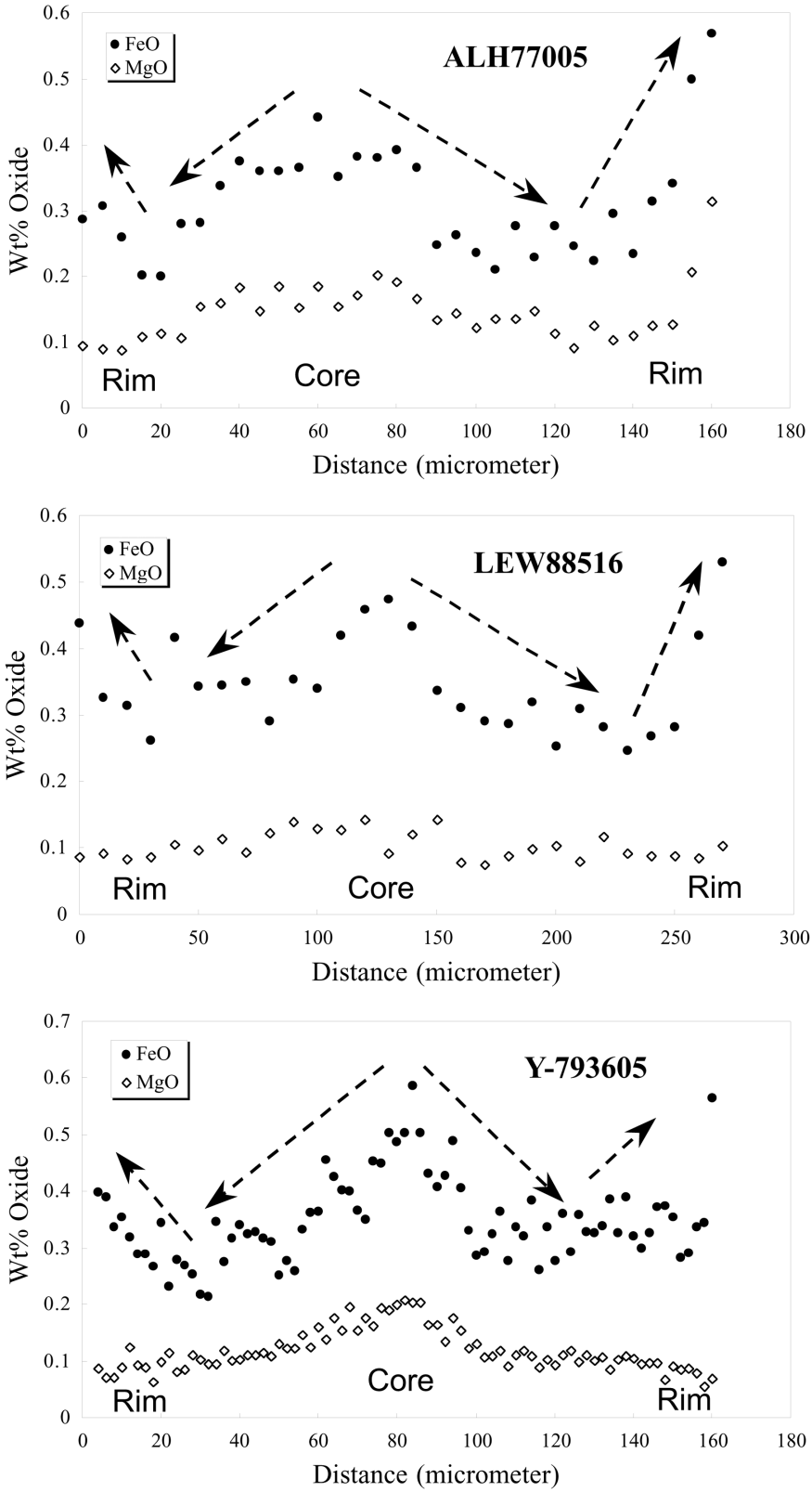

Fig. 15. Fe and Mg zoning patterns in plagioclase glass from lherzolitic shergottites. All of them show similar zoning patterns that both Fe and Mg decrease at first and then increase.

one another (Mikouchi and Miyamoto 2000) (Figs. 11 and 15). It is likely that the changes of Fe abundance from a decrease to an increase observed in all plagioclase glass in lherzolitic shergottites (Fig. 15) record the same event that happened at the late stages of their crystallization. Thus, it is evident that they experienced a very similar igneous crystallization history and supports the hypothesis that they originated from the same igneous unit on Mars. The shock degrees for all lherzolitic shergottites are very strong, but slightly different from one sample to another. GRV 99027 contains abundant shock melt and recrystallizing plagioclase (Hsu et al. 2004) and appears to show the strongest shock metamorphism among lherzolitic shergottites. ALH 77005 also contains abundant shock-melted areas, but recrystallizing plagioclase is rare. In LEW 88516 and Y-793605 shock melt areas are rare and all plagioclase is "maskelynite." From this point of view, the shock degree of NWA 1950 is similar to LEW 88516 and Y-793605.

CONCLUSIONS

1. NWA 1950 is a new lherzolitic shergottite recently found in Morocco. It shows a typical poikilitic texture (several millimeter-sized pyroxene oikocrysts enclosing cumulus olivine and chromite) with interstitial non-poikilitic areas (olivine, pyroxenes, and plagioclase glass).
2. Olivine in non-poikilitic areas is more Fe-rich and shows a narrower distribution than that in poikilitic areas, suggesting re-equilibration of olivine with evolved interstitial melts. Pyroxenes in non-poikilitic areas are also more Fe-rich than those in poikilitic areas.
3. The crystallization sequence of NWA 1950 minerals is: initial crystallization of olivine and chromite, followed by crystallization of low-Ca pyroxenes growing into a large oikocryst poikilitically enclosing cumulus phases (olivine and chromite). Eventually, small interstitial melts formed between oikocrysts after accumulation, and plagioclase began to crystallize from the melt with pigeonite (then augite) forming non-poikilitic areas.
4. NWA 1950 shows close affinities to previously known lherzolitic shergottites, ALH 77005, LEW 88516, Y-793605 and GRV 99027 in mineralogy and petrology. Olivine composition of NWA 1950 is intermediate between those of ALH 77005-GRV 99027 and those of LEW 88516-Y-793605, but is rather similar to ALH 77005-GRV 99027. It is likely that all of these meteorites originated from the same igneous body on Mars and were ejected by the same impact event. The subtle difference of mineral chemistry (especially olivine composition) is due to different degrees of re-equilibration, probably attributed to different locations in the igneous body.

Acknowledgments–I thank Mr. Bruno Fectay and Ms. Carine Bidaut for the NWA 1950 sample. I also thank Mr. O. Tachikawa and Mr. H. Yoshida for technical assistance during electron beam analyses. The electron microscopy was performed in the Electron Microbeam Analysis Facility for mineralogy at Department of Earth and Planetary Science, University of Tokyo. Constructive reviews by Dr. A. Treiman and an anonymous reviewer improved the quality of the manuscript.

Editorial Handling—Dr. Allan Treiman

REFERENCES

Bischoff A. and Stöffler D. 1992. Shock metamorphism as a fundamental process in the evolution of planetary bodies: Information from meteorites. *European Journal of Mineralogy* 4: 707–755.

Borg L. E., Nyquist L. E., Wiesmann H., and Reese Y. 2002. Constraints on the petrogenesis of Martian meteorites from the Rb-Sr and Sm-Nd isotopic systematics of the lherzolitic shergottites ALH 77005 and LEW 88516. *Geochimica et Cosmochimica Acta* 66:2037–2053.

Crozaz G. and Wadhwa M. 2001: The terrestrial alteration of Saharan shergottites Dar al Gani 476 and 489: A case study of weathering in a hot desert environment. *Geochimica et Cosmochimica Acta* 65:971–978.

Fujino K., Naohara H., and Momoi H. 1990: Direct determination of cation diffusion coefficients in pyroxene. *Eos* 71:943.

Goodrich C. A. 2002. Olivine-phyric Martian basalts: A new type of shergottite. *Meteoritics & Planetary Science* 37:B31–B34.

Goodrich C. A., Herd C. D. K., and Taylor L. A. 2003. Spinels and oxygen fugacity in olivine-phyric and lherzolitic shergottites. *Meteoritics & Planetary Science* 38:1773–1792.

Harvey R. P., Wadhwa M., McSween H. Y., Jr., and Crozaz G. 1993. Petrography, mineral chemistry and petrogenesis of Antarctic shergottite LEW 88516. *Geochimica et Cosmochimica Acta* 57: 4769–4783.

Hsu W. B., Guan Y. B., Wang H. N., Leshin L. A., Wang R. C., Zhang W. L., Chen X. M., Zhang F. S., and Lin C. Y. 2004. The lherzolitic shergottite Grove Mountains 99027: Rare earth element geochemistry. *Meteoritics & Planetary Science* 39:701–709.

Ikeda Y. 1994: Petrography and petrology of the ALH 77005 shergottite. *Proceedings of NIPR Symposium on Antarctic Meteorites* 7:9–29.

McSween H. Y., Jr. 1994. What we have learned about Mars from SNC meteorites. *Meteoritics* 29:757–779.

McSween H. Y., Jr. 2002. The rock of Mars, from far and near. *Meteoritics & Planetary Science* 37:7–25.

McSween H. Y., Jr. and Jarosewich E. 1983. Petrogenesis of the Elephant Moraine A79001 meteorite: Multiple magma pulses on the shergottite parent body. *Geochimica et Cosmochimica Acta* 47:1501–1513.

Meyer C. 2003. Mars meteorite compendium 2003. Houston, Texas: NASA Johnson Space Center. http://www/curator.jsc.nasa.gov/curator/antmet/mmc/mmc.htm.

Mikouchi T. and Miyamoto M. 1997. Yamato-793605: A new lherzolitic shergottite from the Japanese Antarctic meteorite collection. *Antarctic Meteorite Research* 10:41–60.

Mikouchi T. and Miyamoto M. 2000. Martian lherzolitic meteorites Allan Hills 77005, Lewis Cliff 88516, and Yamato-793605: Major and minor element zoning in pyroxene and plagioclase glass. *Antarctic Meteorite Research* 13:256–269.

Mikouchi T., Miyamoto M., and McKay G. 1999. The role of undercooling in producing igneous zoning trends in pyroxenes

and maskelynites among basaltic Martian meteorites. *Earth and Planetary Science Letters* 173:235–256.

Misawa K., Nakamura N., Premo W. R., and Tatsumoto M. 1997. U-Th-Pb isotopic systematics of lherzolitic shergottite Yamato-793605. *Antarctic Meteorite Research* 10:95–108.

Morikawa N., Misawa K., Kondorosi G., Premo W. R., Tatsumoto M., and Nakamura N. 2001. Rb-Sr isotopic systematics of lherzolitic shergottite Yamato-793605. *Antarctic Meteorite Research* 14:47–60.

Misener D. J. 1974. Cation diffusion in olivine to 1400 °C and 35 kbar. In *Geochemical transport and kinetics*, edited by Hoffmann A. W., Giletti B. J., Yoder H. S., Jr., and Yund R. A. Washington, D.C.: Carnegie Institute of Washington. pp. 117–129.

Nagao K., Nakamura T., Miura Y. N., and Takaoka N. 1997. Noble gases and mineralogy of primary igneous materials of the Yamato-793605 lherzolite. *Antarctic Meteorite Research* 10: 125–142.

Russell S. S., Folco L., Grady M. M., Zolensky M. E., Jones R., Righter K., Zipfel J., and Grossman J. N. 2004. The Meteoritical Bulletin, No. 88. *Meteoritics & Planetary Science* 39:A215–272.

Treiman A. H., McKay G. A., Bogard D. D., Mittlefehldt D. W., Wang M.-S., Keller L., Lipshutz M. E., Lindstrom M. M., and Garrison D. 1994. Comparison of the LEW 88516 and ALH A77005 Martian meteorites: Similar but distinct. *Meteoritics* 29: 581–592.

Wadhwa M., McKay G., and Crozaz G. 1999: Trace element distributions in Yamato-793605, a chip off the "Martian lherzolite" block. *Antarctic Meteorite Research* 12:168–182.